Fermi National Accelerator Laboratory

Charm and Beauty Physics at Fermilab

R. Lipton

Fermi National Accelerator Laboratory
P.O. Box 500, Batavia, Illinois 60510

January 1992

Disclaimer

Charm and Beauty Physics at Fermilab

Ronald Lipton

Fermi National Accelerator Laboratory

Abstract

The status of charm and beauty physics studies at Fermilab is reviewed. Data from fixed target experiments on charm production, semi-leptonic decay, and Cabibbo suppressed decays as well as charmonium studies in antiproton annihilation are described. In addition beauty results from CDF and E653 are reviewed and prospects for studies of B physics at collider detectors are discussed.

Hadronic production of heavy quarks has long held the promise of very high statistics samples of charm and beauty. With the current generation of charm experiments this promise is now being fulfilled. Experiments have also taken the first steps toward studies of beauty in fixed target and collider experiments. In this report we present an overview of the current state of charm and beauty studies at Fermilab and comment on expectations for the 1990's[1].

I. Fixed Target Charm.

Charm experiments at Fermilab began soon after the discovery of the J/Ψ at SLAC. Charm production and decay has been studied using hadron, photon as well as neutrino beams. The program has evolved substantially, continuing to incorporate developments in experimental technology. Crucial developments include:

- Secondary vertex detection using silicon strip detectors. These devices can improve the signal/noise by factors of more than 100. They also make possible measurements of lifetimes.
- High rate data acquisition systems. The data acquisition system in E791 can write ~10,000 events per second to tape. These systems are complemented by off line computing farms which have the ability to analyze the billions of events collected.

- Sophisticated trigger processors. Some experiments (E690,E789) have chosen to use very high throughput track reconstructing trigger processors to select charm and beauty events.

These capabilities give the experiments involved in the current fixed target run the ability to collect samples of charm decays with an order of magnitude more reconstructed decays than previous generations.

Ia. Current Experiments

Fixed target experiments are in progress using photon and hadron beams. The experimental framework for the two environments differ. In photoproduction the topology is semi-diffractive. Typically photoproduced charm events have low primary multiplicity and charm pairs which carry a large fraction of the beam momentum . The charm pair production cross section is about 1% of the hadroproduction rate (1 μb / 120 μb) . The low primary multiplicity and lack of a beam track means that primary vertex reconstruction is more difficult in photon beams than in hadronic production experiments. On the other hand the relatively large signal/background ratio means that most photon beam experiments can run with a loose trigger and data reduction can proceed more quickly.

In hadroproduction the signal/background, $\sigma(\pi p \rightarrow C \bar{C} X)/\sigma(\pi p \rightarrow X)$, is about 0.1% (30μb /40 mb), a factor of 10 smaller than in photoproduction. In addition much of the yield is at low X_F, with production parameterized as $(1-X)^3 - (1-X)^7$ depending on beam momentum and composition (π or proton). Typical hadroproduction studies are high rate, triggered experiments. An exception is E791, which substitutes a very high rate data acquisition system for a restrictive trigger.

Table 1 summarizes the experiments with new results. E687 has results from a brief run in 1987-88, E769 has studied charm production as a function of beam and target, E691 continues it's impressive yield of physics results, and E653 has results on charm production and semi-leptonic decay physics.

Table 1: Fermilab Charm Experiments

E687 Photoproduction (wide Band)
  Wide band photon beam < Eγ > ~ 220 GeV
  Open Trigger
  Silicon μ-strip system (8,400 channels)
  Results from 1987-88 run (60×10^6 Trig)
  Currently running (Already > 270×10^6 Trig)

E691(γ),E769(π,K,p),E791(π)
  E$_T$ Trigger
  E691 - Photon Beam (1985)
  E769 - 250 GeV hadron beam (1987) - Production, A dependence
  E791 - 500 GeV hadron beam
      Very high rate data acquisition (10,000 events/sec)

E653(p,π)
  Hybrid Emulsion experiment
  800 GeV p - 1985
  600 GeV π - 1987
  Beauty and Charm results, electronic and emulsion analysis
  Short Spectrometer, μ trigger

E690(p)
  On line event reconstruction
  Study of diffractive charm production in target fragmentation

Currently E791, E690 and E687 are taking data. E791 and E687 expect more than 100,000 reconstructed charm events from this run (ten times current samples from experiments like E691). E690 will study diffractive charm production using an on line trigger processor. In the future E781, a completely new experiment, will study high X baryon production from hyperon beams. It is worth noting that few of the most impressive results from E691 and E653 were anticipated in the proposals. Data makes us more creative.

Ib. Production Results

There are new results from E653 and E769 on the characteristics of hadronic charm production. Hadronic production is usually parameterized as:

$$\frac{d^2\sigma}{dX_f dP_T^2} = (1-X_f)^n \ e^{-bP_T^2}$$

Results from pion and proton beams now span the range from $\sqrt{s} = 20\text{-}38$. Both E653[2] and E769[3] have preliminary results. Figure 1 shows the new results along with a compilation of previous Fermilab and CERN data[2][4]. B, the p_T slope, ranges between .8 and 1.3 GeV^{-2} and does not appear to have any strong energy dependence. The values for n found in pion beam experiments range from 3 to 4.5 and also show little variation with energy. The proton data lies above the pion results and the value of n appears to increase with $\sqrt{s}$.

Recently preliminary next-to-leading order QCD calculations have become available for charm production in pion beams[5]. The $(1-X)^n$ form fits both leading order and next to leading order calculations quite well[2]. The value of n for next-to-leading order QCD is .6 lower than the leading order number. The prediction of the next-to-leading order calculation for $\sqrt{s} = 34$ is quite close to the E653 data point (4.69 vs 4.2±0.2). Charm production is a low q^2 process where the QCD calculations are marginal and no attempt is made to include fragmentation or nuclear effects in the calculation. In this context the agreement between theory and experiment is quite satisfactory.

Evidence from early hadronic charm production measurements in beam dump experiments had suggested that the production cross section might have a nonlinear A dependence[6][7], A^α, with $\alpha \sim .77$. These results implied that some unexpected nuclear effects might occur in heavy quark production. E769 has measured α to be 0.97±0.07 for $D^\pm$ and 0.92±0.08 for D^0, consistent with quark model expectations of $\alpha=1$.

E653 results on charm pair production[8], and photoproduction results[9] have not been discussed. In the near future E791 should provide a wealth of data on charm

production at $\sqrt{s}$ = 31. E653 will have results on approximately 1000 charm pairs found in emulsion scanning, and E687 will have improved photoproduction data.

Ic. Hadronic Charm Decay

The big surprise in charm physics, the difference in D^0 and D^+ lifetimes, is still not completely understood. Experiments are beginning to accumulate enough data on specific decay modes to sort out the details of hadronic decay mechanisms. Both W exchange and interference effects contribute to the lifetime difference. Final state interactions also play a large role in charm decays. One approach to studying these effects is to select decays where specific diagrams, such as the W exchange, are expected to be dominant.

A number of new results are available on hadronic decays from E687 and E691. An example is the (preliminary) E687 [10] measurement of $D^0 \rightarrow K_s\phi$ (figure 2). This decay is dominated by W exchange and final state interaction contributions. The E687 signal is shown in figure 3. The measured branching ratio is $B(D^0 \rightarrow K_s\phi)$ = $0.77\pm0.37\pm$ 0.58%. The average of previous CLEO, ARGUS and MARK III results is $0.83^{+0.18}_{-0.16}$ %. Table 2 compares E687 and e^+e^- results to predicted values.

Table 2: Comparison of experimental results to models.

Model	$B(D^0 \rightarrow K_s\phi)$
Spectator	~0%
BSW	0.75%
QCD sum rules	1.3%
E687	0.77± .37 %
Average of CLEO, ARGUS, MARK III	$0.83^{+.18}_{-.16}$%

Another example of this sort of study is the Cabibbo suppressed decay $D^0 \rightarrow K^*K$. In this case E691 [11] studied D^0 decay to the final states $K^{*+}K^-$, K^+K^{*-}, $K^{*0}\bar{K}^0$ (plus the charge conjugate $\bar{D}^0$ states). As can be seen from figure 4; in the absence of W exchange and interference the final state should be dominated by $K^{*+}K^-$. The various

K*K modes all have identical phase space and form factors so any difference in rate should reflect the underlying dynamics.

E691 measurements are summarized in table 3. As expected the spectator modes dominate, with little signal seen in the modes dominated by exchange or the mode where the vector meson is identified with the spectator quarks.

Table 3: E691 Measurements of K*K decays

Decay Mode	$\dfrac{BR(D^0 \to f) \times 100}{BR(D^0 \to K^- \pi^+)}$	Comment
$K^{*+} K^-$	$.16\,^{+0.08}_{-0.06}$	Spectator diagram, W$\to$vector
$K^+ K^{*-}$	$.00\,^{+0.03}_{-0.00}$	Spectator diagram, spectator$\to$vector
$K^{*0} \bar{K}^0$	$.00\,^{+0.04}_{-0.00}$	Exchange + final state interactions

Table 4 summarizes recently published results on Cabibbo suppressed decays from E691 and preliminary results from E687. These studies are only beginning. Future data from E687 and E791 should be sensitive to .1% branching ratios for many of these rare modes. New results which I have not discussed include E691's limit on direct CP violation in D decay[12], and E687's measurements of charm lifetimes and D^0 mixing[13].

Table 4: Recent results on Cabibbo suppressed decays.

E691 Results

Decay Mode	$\dfrac{BR(D^0 \to f) \times 100}{BR(D^0 \to K^-\pi^+)}$	Branching Ratio(%)
K^+K^-	$.114 \pm .011 \pm .009$	
$\pi^+\pi^-$	$.059 \pm .009 \pm .005$	
Inclusive $K^0K^-\pi^+$	0.16 ± 0.06	$0.69^{+0.27}_{-0.23} \pm 0.14$
$\bar{K}^{*0}K^0$	$.00^{+0.03}_{-0.00}$	<0.13
$K^{*+}K^-$	$.16^{+0.08}_{-0.06}$	$0.69^{+0.32}_{-0.26} \pm 0.15$
Nonresonant $K^0K^-\pi^+$	0.06 ± 0.06	<0.53
Inclusive $\bar{K}^0 K^+\pi^-$	0.10 ± 0.05	$0.42^{+0.23}_{-0.20} \pm 0.09$
$K^{*0}K^0$	$.00^{+0.04}_{-0.00}$	<0.22
K^+K^{*-}	$.00^{+0.03}_{-0.00}$	<0.17
Nonresonant $\bar{K}^0 K^+\pi^-$	$.10^{+0.06}_{-0.05}$	$0.42^{+0.23}_{-0.20} \pm 0.09$

	$\dfrac{BR(D^0 \to f) \times 100}{BR(D^0 \to K^-\pi^+\pi^-\pi^+)}$	
Inclusive $K^+K^-\pi^+\pi^-$	$2.8^{+0.08}_{-0.07}$	$0.26^{+0.07}_{-0.06} \pm 0.05$
$\phi\,\pi^+\pi^-$	$.76^{+0.66}_{-0.49}$	<0.15
$K^{*0}\bar{K}^{*0}$	$3.6^{+2.0}_{-1.6}$	$0.33^{+0.18}_{-0.15} \pm 0.07$
Nonresonant $K^+K^- \pi^+\pi^-$	$0.1^{+1.1}_{-0.1}$	<0.14

E687 Results

Mode	Branching ratio
$D^0 \to \pi^+\pi^+\pi^-\pi^-/K\pi\pi\pi$	$0.10 \pm .02 \pm .02$
$D^0 \to \pi\pi/K\pi$	$0.12 \pm .03$
$D^0 \to \bar{K}^0 K^+K^-/ \bar{K}^0 \pi^+\pi^-$	$0.198 \pm 0.057 \pm 0.78$
$D^0 \to \bar{K}^0 \phi / \bar{K}^0 \pi^+\pi^-$	$0.121 \pm 0.057 \pm 0.090$
$D^0 \to \bar{K}^0 (K^+K^-)_{non\,\phi}/ \bar{K}^0 \pi^+\pi^-$	$0.136 \pm 0.042 \pm 0.068$
$D_s \to \phi \pi^+\pi^-\pi^+/ \phi \pi^+$	$0.58 \pm 0.20 \pm 0.10$

Id. Semi-Leptonic Charm Decay

Semi-leptonic decays provide clean tests of the quark model. Weak interaction effects in these decays are well understood, and form factors and decay rates test quark model and QCD predictions. In addition the strong association between form factors in semileptonic B and C decays means that the charm data can be used to test our understanding of the factors that influence B$\rightarrow$ C$l\nu$ decay and therefore B$\rightarrow$ u rates. The rather simple structure of the matrix elements and form factors should ultimately allow a complete description of charm semileptonic decays.

Both E691[14] and E653[15] have reported new results on the decay D $\rightarrow$ K$^{\pm,0}l\nu$. E691 had earlier reported results on the rate for D^0 $\rightarrow$ K$^{\pm}$ev, using D* decays to tag the D^0 [16]. The rate for decays with additional unobserved neutrals such as D^0 $\rightarrow$ K$^{\pm}\pi^0$ev are calculated from the observed K*^{0}ev rate. The new result reports on the D$^+$ $\rightarrow$ K^{0}ev rate which, by isospin, should equal the K$^{\pm}$ev rate. The experimental signature is a K^0 plus an electron with a large impact parameter. There are no reconstructable vertices in these decays and the result reflects a detailed understanding of backgrounds in the E691 detector.

E653 has reported results on D^0 $\rightarrow$ K$^{\pm}\mu\nu$ using a different technique. Two prong semi-muonic vertices are found in the emulsion. Good knowledge of the parent direction allows them to form the "minimum parent mass":

$$M_{min} = \sqrt{m_{vis}^2 + p_t^2} + p_t$$

This distribution is sharply peaked for decays with one missing neutrino (such as D^0 $\rightarrow$ K$^{\pm}$ev) but is shifted down and widens for decays such as D^0 $\rightarrow$ K$^{\pm}\pi^0$ev. A fit to the shape of the M$_{min}$ distribution provides the fraction of events with a single missing neutrino. Table 5 summarizes the current data from E653, E691, Mark III and CLEO. Recent E691 and E653 data agree and have brought the word average for the width down a bit to 7.2±0.6x10^{10} sec^{-1}. New data from all electronic analysis of E653 and E687 should substantially improve the quality of the data.

Table 5: D → $K^{\pm,0}l\nu$ rates (10^{10} sec.$^{-1}$)

Experiment	$D^+ \to K^0 l\nu$	$D^0 \to K^\pm l\nu$
Mark III	5.6±.65(e)	8.1±1.2±1.0 (e)
	6.6±1.1(μ)	
E653		**5.6±.9±1.2** (μ)
E691	**5.6±0.8±1.5** (e)	9.1±0.7±1.4(e)
CLEO		8.8±0.7±1.4(e)
		7.8±0.9±1.4(μ)
Average		7.2±0.6

There are also new results for E653[17] and E691[18] on $D^\pm \to K^* l\nu$ form factors and polarization. The form factors are obtained from a fit to the the K* decay angular distributions:

$$d\Gamma \sim G_F{}^2 \, |V_{cs}|^2 \, B(q^2)[sin^2\theta_V(1+cos\theta_l)^2 \, H_-{}^2 + sin^2\theta_V(1-cos\theta_l)^2 \, H_+{}^2 + cos^2\theta_V sin^2\theta_l \, H_0{}^2]$$

$$H_+ \sim A_1(q^2)(M_D+M_{K\pi}) + B_1(q^2)\frac{V(q^2)}{(M_D+M_{K\pi})} \quad \text{Transverse amplitude}$$

$$H_0 \sim B_2(q^2)A_1(q^2)(M_D+M_{K\pi}) - B_3(q^2)\frac{A_2(q^2)}{(M_D+M_{K\pi})} \quad \text{Longitudinal amplitude}$$

Where θ_V is the polar angle in the K* frame between K$^-$ and the direction opposite the D$^+$ and θ_l is the angle in the W frame between the lepton and the direction opposite the D$^+$; A_1,A_2,V are the form factors and the B's are kinematic factors. E691 has reported measurements of both the polarization (Γ_L/Γ_T) and overall rate ($4.2 \pm 0.6 \pm 0.5 \times 10^{10}$ sec^{-1}). CLEO ARGUS and MARK III measurements for the rate agree well with E691. E653 has only measured form factor ratios and does not yet have results for the semileptonic decay rate. The $K\pi$ mass distribution for semileptonic three prongs in E653 is shown in figure 5. Figure 6 presents the observed θ_V distribution and results from the form factor fit. Results for the form factors and ratios are summarized in table 6.

Table 6: D → K*lν Form Factors and Ratios at $q^2 = 0$

Ratios	$A_2(0)/A_1(0)$	$V(0)/A_1(0)$	Γ_L/Γ_T
E653	0.69±0.23	1.99±0.31	1.2±0.2
E691	0.0±0.5±0.2	2.0±0.6±0.3	$1.8^{+0.6}_{-0.4}\pm0.3$
Theory	0.1 → 1.3	0.8→ 2.0	0.9 → 1.7
Form Factors	$A_1(0)$	$A_2(0)$	$V(0)$
E691	0.46±0.05±0.05	0.0±0.2±0.1	0.9±0.3±0.1
Theory	0.8→1.0	0.6→1.0	1.0→1.5

E653 and E691 values for the form factor ratios are in acceptable agreement, with E653 measuring a larger value for A_2/A_1 and therefore a smaller value for the polarization, Γ_L/Γ_T. There has been a great deal of theoretical work on this subject including predictions using quark models, lattice gauge calculations, and QCD sum rules. Many models can accommodate the range of measured form factor ratios. Quark model calculations do not easily accommodate the rate measured by E691, and in general the lattice and QCD sum rule calculations seem to provide a better overall description of the data than the existing quark model calculations[19].

Finally both E687 and E653 have preliminary signals in the $D_s \to \phi\mu\nu$ channel. The E653 data is shown in figure 7. E653 is in the process of measuring these events in the emulsion.

Ie. Charmonium Production in $\bar{p}p$ annihilation.

Only charmonium states with $J^{pc} = 1^{--}$ are directly produced in e^+e^- annihilation. A new Fermilab experiment, E760[20][21], uses a stochasticaly cooled ($\Delta p/p_{rms} = 2\times10^{-4}$) antiproton beam and an internal gas jet target in the Fermilab Accumulator to study $\bar{p}$ p → $\bar{c}$ c in all allowed J^{pc}. The physics program includes the precise study of χ states, measurement of $\eta_c \to \gamma\gamma$, confirmation of the $\eta_c'(0^{-+})$, a search for the predicted narrow states ($^1P_1(1^{+-}),^1D_2(2^{-+}),^3D_2(2^{--})$), and a search for new resonances. Angular

distributions of radiative decays of $\bar{c}c$ states, helicity amplitudes, and multipole structures are also on the menu.

The technique follows an earlier CERN ISR experiment[22], but with a center of mass energy spread of 250 KeV, 3-4 times smaller than that achieved in the ISR. A basic constraint in the $\bar{p}p$ annihilation technique is the small value of σ(signal)/σ(total) ~ 10^{-6} . With this large background triggering and background rejection are crucial. The detector is a non magnetic spectrometer with Cerenkov particle identification and lead glass calorimetry. E760 concentrates on electromagnetic final states ($e^{+}e^{-}$, γγ), which are well measured and have small backgrounds.

The masses and widths of the χ states were rather poorly known before the 1990 run of E760. The basic technique used in E760 for the study of χ states is to measure the rate for for $\bar{p}\,p \rightarrow X \rightarrow \gamma\,J/\Psi$, $J/\Psi \rightarrow e^{+}e^{-}$ as a function of center of mass energy. The J/Ψ yields in the χ_1 and χ_2 regions are shown in figure 8. First run results for the χ and J/Ψ are given in table 7. Errors on mass measurements of the χ states are more than a factor of two smaller than those of previous measurements. As can be seen from the table the improvements for the widths are even more substantial.

Table 7: $\overline{C}C$ Resonance parameters for 1990 data of E760.

Resonance	Mass(MeV/c^2)	Width(KeV)
J / ψ (E760)	3096.88 ± 0.06 ± 0.03	
J / ψ (PDB)	3096.93 ± 0.09	63 ± 9
χ_1 (E760)	3510.53 ± 0.04 ± 0.12	880 ± 110 ± 80
χ_1 (PDB))	3510.6 ± 0.5	<1300
χ_2 (E760)	3556.15 ± 0.07 ± 0.12	1980 ± 170 ± 70
χ_2 (PDB)	3556.3 ± 0.4	2600^{+1200}_{-900}
ψ' (E760)	3686.0 (input)	
ψ' (PDB)	3686.0 ± 0.1	243 ± 40
χ_1 - χ_2	45.62 ± 0.08 ± 0.07	

II. Beauty Physics - Fixed Target

IIa. E653

There are new B pair production results from E653, a fixed target hybrid emulsion experiment. Previously there had been only one reconstructed B pair found in a fixed target experiment[23] and a cross section derived from trimuon production in a 320 GeV π beam[24]. E653 differs from previous B studies in that all decay vertices are unambiguously reconstructed and charged tracks are momentum analyzed.

The data were taken in the 1987 run of E653 with a 600 GeV pion beam incident on an emulsion target. Events with muon transverse momentum greater than 1.5 GeV/c were selected for scanning in the emulsion (Scan 1) this scan is almost complete. Events with muon $p_T>0.8$ GeV/c and hadron $p_T>1.0$ GeV/c are currently being scanned (scan 2).

The scanning technique is shown schematically in figure 9. In scan 1 there were 6320 scanning candidates. Of these all but 353 had the muon track slope matched to a track emerging from the primary vertex. These events were rejected in less than 10 minutes. For events with the muon unmatched to the primary vertex all emulsion tracks

with no spectrometer match were followed down through the emulsion block to look for charged decays. In addition tracks reconstructed in the spectrometer with no match to emulsion tracks from the primary vertex were scanned back from the emulsion exit to search for neutral decays.

Twelve B pair events with at least one decay in the emulsion target have been found. Nine are from scan 1, three were found so far in scan 2. The events have the following characteristics:

- All are <u>pairs</u>
- 4 B$\rightarrow$D*
- 1 B $\rightarrow$ J/ψ X, J/ψ $\rightarrow$ $\mu\mu$
- 1 B $\rightarrow$ D$_S$ $\rightarrow$ $\phi\mu\nu$, $\phi\rightarrow$KK candidate
- 1 Charmless decay candidate

E653 has evaluated the production characteristics for the 10 B pair sample available in midsummer. Figures 10 and 11 show the X_f and p_T^2 distributions for the B candidates. Results of a fit to X_F and P_T dependence are:

$$\frac{dN}{dX_F} = (1 - |X_F - 0.075|)^n \quad n = 3\,^{+0.9}_{-0.6}$$

$$\frac{dN}{dP_T^2} = e^{-bp_T^2} \quad b = 0.08\,^{+0.02}_{-0.01}$$

It is clear that the p_T^2 dependence is stiffer in beauty production than that for charm, where b is about one. The calculated cross section is $\sigma = 30\,^{+10}_{-14}\,^{+9}_{-5}$ μb, in agreement with QCD predictions[25]. For the 20 B candidates included in E653's current analysis the overall lifetime is $1.65^{+0.6}_{-0.4}$ ps. The 12 neutral decays have a lifetime of $0.95^{+0.5}_{-0.3}$ ps and the eight charged decays have a lifetime of $2.5^{+2.0}_{-0.8}$ ps. The charged lifetime is heavily influenced by one long decay (8 ps). These results are preliminary and E653 *does not* claim to have observed unequal charged and neutral lifetimes.

IIb. Current Fixed Target B Experiments:

There are currently two fixed target experiments, E789 and E771, dedicated to exploring B physics. Both use modifications of previously existing detectors to explore possibilities for fixed target B physics. The E653 measurements indicate that the B cross section is about $30nb/40mb \sim 10^{-6}$ of the total cross section. In addition the B decay branching ratios into typical reconstructable modes such as $\psi(\rightarrow\mu\mu)K^*$ are small, typically a few $\times 10^{-5}$.

E789 uses the existing E605 apparatus, a very high rate two arm spectrometer which was previously used to study high mass dihadron and dilepton states. The idea here is to use a very high rate system ($>10^8$ interactions/sec) with moderate acceptance ($\sim 1\%$ for $B\rightarrow\pi\pi$), and vertex reconstruction to provide an acceptable B yield and trigger rate. The two arm spectrometer is most sensitive to two body decays such as $B\rightarrow\pi\pi$. This charmless decay is a major goal of the experiment. Other physics goals include:

Measure $B \rightarrow \psi X$
Measure $B \rightarrow K\pi$, KK, $\Lambda_b\rightarrow p\pi$ *(measure $B \rightarrow u$)*
Measure $D^0 \rightarrow K\pi$, KK, $\pi\pi$, $\mu\mu$

Substantial issues of accidentals, trigger rates, and reconstruction all must be understood before the experiment can run at the high rates necessary. The collaboration is currently running with their silicon vertex detector and expects "high rate" data in 1994.

E771 use a modification of the existing E705 spectrometer with a silicon microstrip system. This experiment is a large acceptance forward spectrometer, in contrast to E789. Their focus is on measurements of $B \rightarrow \psi K_s$. Sensitivity is achieved by a high rate system (2×10^6 -10^7 interactions/sec), a dimuon trigger, and a high rate vertex detector. Physics goals include measurement of the CP flagship decay $B \rightarrow \psi K_s$ as well as branching ratios, lifetimes, B_s, and Λ_b. Again the challenges include the very high interaction rates, radiation damage in silicon, triggering, and background rejection.

Both E687 and E791 intend to extend their studies, which now concentrate on charm, to beauty physics in the next fixed target run.

III. Collider B Physics

IIIa. Framework

We first discuss the framework for experiments looking for beauty at the Fermilab collider. At collider energies the cross section is substantially increased:

$$\frac{\sigma(\bar{p}p \rightarrow \bar{B}B\ X)}{\sigma(tot)} \sim \frac{40\ \mu b}{60\ mb} \sim .1\% \text{ (about equal to fixed target charm)}$$

So at a typical value of main injector luminosity of 10^{31} about 400 B pairs are produced per second. Yield is not the problem. Production kinematics and reconstructability drive experimental design. At the collider the bulk of B production is forward and soft (figure 12). Experience with charm shows that vertex reconstruction is crucial, so we would like $\gamma > 2$ to give reasonable values of decay lengths and multiple scattering errors. Most current collider experiments take data at only a few Hertz. Data acquisition upgrades are possible, but CDF and D0 will probably saturate at a few 10's of Hertz. Given the large B rate, a trigger which selects B events useful for physics analysis is important. D0 studies indicate that single muon triggers are viable at $\eta < 2$. For the important B$\rightarrow$$\psi$ mode, dilepton triggers may be viable at $\eta < 2.5$-3.

IIIb. CDF Results

CDF has extremely encouraging results for B physics at hadron colliders. B physics was of "secondary importance" in the 1988/1989 CDF run. There was no silicon vertex detector and little emphasis on low p_T triggers. However substantial results have emerged from three data samples: inclusive electrons, inclusive J / ψ $\rightarrow$ $\mu^+\mu^-$, and e μ. The CDF data will be reviewed briefly since these results have been presented elsewhere[26] and will also be discussed by Dr. Patrick. The data are not only important in their own right but serve as a basis from which to extrapolate to the future.

Figure 13 shows the electron candidate p_T spectrum from the central pseudorapidity region ($\eta < 1$). The electrons come from two data samples, one with an E_T threshold

of 12 GeV, and a second, prescaled sample, with a 7 GeV threshold. Calculations based on the ISAJET Monte Carlo indicate that most of these electrons come from beauty decay (see table 8). CDF has verified this by reconstructing a sample of $D^0 \rightarrow$ $K\pi$ and showing that the bulk of the events have the correct sign (kaon charge same as electron charge).

Table 8: Sources of electrons in CDF sample after W/Z subtraction (ISAJET):

Source	$B_{u,d}$	B_s	B	C	Seq C	J/ψ
%	72	12	5	9	2	1

The dimuon data sample consists of muons with $p_T > 3$ GeV. A clear J/ψ signal is seen. This sample is used to search for $B \rightarrow J/\psi$ (K^*,K) using the following procedure:

> Mass constrain the J/ψ.
>
> Select tracks in 60° cone around the J/ψ.
>
> Require that for $K^{\pm}$ candidates the p_T of the K is greater than 2 GeV
>
> For K^* candidates require $M_{K\pi}$ within 50 MeV of K^*, $K\pi$ among 3 highest p_T
>> tracks

The resulting invariant mass distribution is shown in figure 14.

CDF has used these data to calculate a beauty cross section for $p_T > 10$ GeV. The production cross sections from $B \rightarrow J/\psi$ K are:

$$\sigma(\bar{p}\, p \rightarrow bX; \, p_T > 10 \text{ GeV, } |y|<1.) = 8.2. \pm 2.9(\text{stat}) \pm 3.3(\text{syst}) \, \mu b$$

Cross sections from inclusive electron data are given in table 9.

Table 9: CDF B production cross sections for inclusive electron data.

p_T^e	$p_T^b > p_T^{min}$	σ_b(nb)
10-15	15	1220±390
15-20	23	220±70
20-25	32	56±18

IIIc. The Near Future

The CDF data form a basis for extrapolation to future runs better suited for B physics. A glance at figures 12 and 13 shows that the acceptance for B decays in the 1988 CDF configuration was not optimal. Upgrades to the CDF trigger and muon systems aim to lower p_T thresholds, improve resolution at the trigger level, reduce backgrounds (such as punchthrough), and increase coverage. For the 1992-93 run the integrated luminosity will increase by a factor of 6-10. Plans are underway to optimize the CDF trigger for a lower p_T threshold for muons ($3 \rightarrow 1.8$ GeV) from dimuon events and a reduced electron p_T threshold of ~ 9 GeV. The combination of these upgrades is expected to increase the B yield by a factor of 25-150. In addition CDF will install a four layer silicon vertex detector (SVX). The SVX will provide tracking and vertexing information (in r-ϕ) to $\eta=1.9$. Yields expected for the 1994-95 period are:

3×10^6 semileptonic B decays to tape

400-2400 B $\rightarrow \psi$ K$^{\pm}$ (The 1987 sample is about 15)

400-2400 B $\rightarrow \psi$ K*

150-500 B$_S \rightarrow \psi \phi$

40-200 $\Lambda_b \rightarrow \psi \Lambda$

CDF is expected to study B$_S$ production and decay, identify B baryons, and work with samples of several million semileptonic decays.

D0 will have it's first run in 1992. D0 boasts excellent calorimetry and lepton identification. As can be seen from the dotted line in figure 12 , muon coverage in D0 is more extensive than in CDF. D0 expects to be able to trigger on muons well beyond $\eta=1.5$, and dimuons down to $\eta=2.5$. This capability means that D0 should be able to extend B cross section and production measurements to lower p_T. D0 has no central magnetic field so that studies of exclusive final states are difficult. However the excellent muon identification will allow detailed inclusive B $\rightarrow \psi$ studies and decays which can be identified topologically such as B $\rightarrow \psi$ K$_S$,Λ.

IIId. B Physics in the Main Injector Era:

The main injector is expected to be completed in 1997. the main injector is a completely new environment for collider physics. Luminosity will increase a factor of

~50 from the current value of 10^{30} to 5 x 10^{31}. The collision interval will be reduced from 3.5 µs to 395 ns. Both D0 and CDF will need extensive upgrades to operate in this high luminosity, short crossing interval environment. The CDF upgrade as currently envisioned is evolutionary[27], with upgrades to the µ system, SVX and the trigger. The D0 upgrade plan is more ambitious[28], converting from a non-magnetic to a magnetic detector by adding a superconducting solenoid. The tracking upgrade aims to maintain D0's excellent overall coverage. Vertices are found in a silicon barrel/disk system with acceptance to η=3 and a scintillating fiber tracker is used for tracking and momentum measurement. The scintillating fiber system will use 800 µm fibers (XUV) read out using cryogenically cooled visible light photon counters, which have an 85% quantum efficiency. The system is well matched to the characteristics of B production. Both existing collider detectors intend to pursue B physics while continuing to study high p_T physics. Physics goals include B_s mixing, rare B decays, B spectroscopy, and CP violation.

As an example of the reach of collider experiments in the main injector era we consider the CP violation benchmark decay B → ψ K_S. The goal is to measure the Unitarity Triangle angle β.The time evolution of a B^0 decaying into ψ K_S is:

$$N_{B^0(t)} = \int_0^t e^{-\Gamma t}(1+\sin 2\beta \sin x \Gamma t)\, dt \rightarrow \frac{1}{\Gamma}(1+\frac{x}{1+x^2}\sin 2\beta)$$

$$N_{\bar{B}^0(t)} = \int_0^t e^{-\Gamma t}(1-\sin 2\beta \sin x \Gamma t)\, dt \rightarrow \frac{1}{\Gamma}(1-\frac{x}{1+x^2}\sin 2\beta)$$

Here Γ is the total width and x is the mixing rate, $\frac{\Delta m}{\Gamma}$, where the formulas to the right of the arrows assume that the time evolution is not observed. Assuming all B^0's are tagged at birth the asymmetry is:

$$A = \frac{N(B^0)-N(\bar{B}^0)}{N(B^0)+N(\bar{B}^0)} = \frac{x}{1+x^2}\sin 2\beta$$

where the factor $\frac{x}{1+x^2}$ is the dilution factor coming from the integral over time. Additional dilution arises from mistagging the B. In the model experiment it is assumed

that the lepton from the partner B is used to tag the B^0. In this scenario the dilution factor must include backgrounds due to semi-leptonic cascade charm decays, π and K decay, and hadronic punchthrough. The overall error in sin 2β is:

$$\delta(\sin 2\beta) = \frac{1}{D \sqrt{N}}$$

where D is the total dilution factor and N is the number of tagged events.

D0[29][30] and CDF have studied the sensitivity of their upgraded detectors to sin 2β. In the D0 study an attempt was made to optimize the lepton p_T cuts to minimize the luminosity needed for a given error in sin 2β. The dilution factor was found to be .21.

Table 10 compares B yields projected for two fixed target experiments expected to run in 1994 with CDF expectations for the next two collider runs and with expectations for both collider experiments in the main injector era. For each experiment a representative decay mode has been chosen. A few points are worth noting: The two fixed target experiments (E789, E771) achieve sensitivity by very high luminosity, E789 hopes for a factor of 400 over CDF in the same time period. However, the factor of about 1000 in cross section between the collider and fixed target experiments means that the yield of B events is similar (within the errors of the estimate). E771 and E789 trade rate for acceptance and end with comparable statistics. In the near future high rate fixed target experiments can be competitive with collider B studies only if they succeed in operating at very high rates. The increased luminosity at the main injector favors collider B physics toward the end of the decade.

Following reference 30 I have extended the table for D0 to include expectations for measurement of CP violation. The calculated error in sin 2β is .17. The anticipated value is about .3 so the expected range for the upgraded D0 may be interesting. Is it really achievable? We will know much more after the next collider run.

Table 10: Summary of expectations for Benchmark decays from B experiments

	D0 Upgrade	CDF Upgrade	CDF 1992	E771 1994	E789 1994
Mode	$B \to \psi K_S$	$B \to \psi K_S$	$B \to \psi K_S$	$B \to \psi K_S$	$B \to \pi\pi$
Luminosity	5×10^{31}	5×10^{31}	5×10^{30}	5.0×10^{31}	2.0×10^{33}
Time (sec)	1.0×10^7	1.0×10^7	1.0×10^7	1.0×10^7	1.0×10^7
Int Luminosity	5×10^{38}	5×10^{38}	5×10^{37}	5.0×10^{38}	2.0×10^{40}
B pair cross section	$40 \mu b$	$40 \mu b$	$40 \mu b$	10 nb	10 nb
B0 Fraction	0.75	0.75	0.75	0.75	0.75
Trigger eff x acceptance	0.027	0.015	0.010	0.320	0.0045
Target BR	2.5×10^{-5}	2.5×10^{-5}	2.5×10^{-5}	2.5×10^{-5}	1.0×10^{-5}
Yield to Tape	9954.	5625.	375.	25.	8.
Tagging eff.	0.087				
Tagged Events	866				
Dilution factor	0.2				
$\delta(\sin 2\beta)$	0.17				

IV. Conclusions

Charm studies at Fermilab are a mature field with compelling results from previous runs and hundreds of thousands of reconstructed decays expected from the current run. E791 is well on the way to collecting more than 10^{10} triggers. When these data are analyzed well over 200,000 reconstructed decays will be available. Figure 15 shows results of E687's analysis of 4.5 hours of data taken during the 1991 run. B physics at Fermilab is just beginning. E653 and CDF have provided valuable experience and demonstrated the potential for beauty studies at Fermilab. The current experimental challenge is to learn to study B physics with quality and sophistication comparable to the charm physics program.
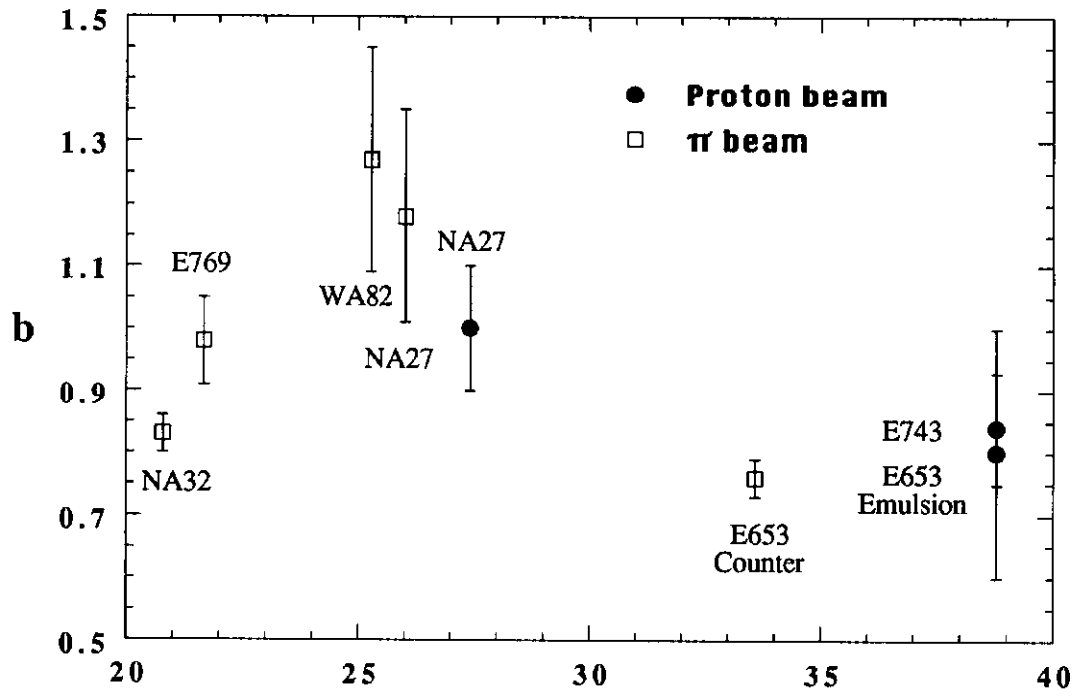
Figure 1a. P_T slope as a function of E_{cm}
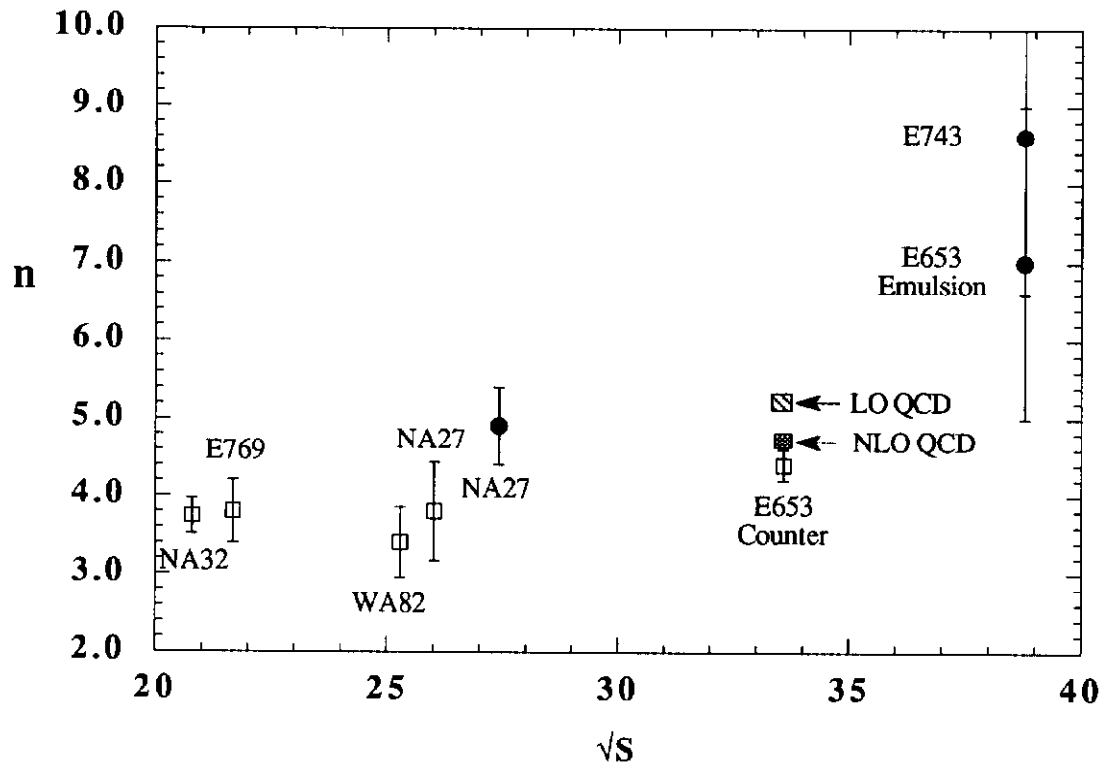
Figure 1b. n as a function of E_{cm}
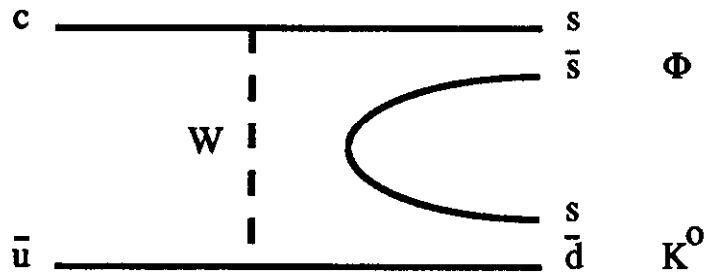
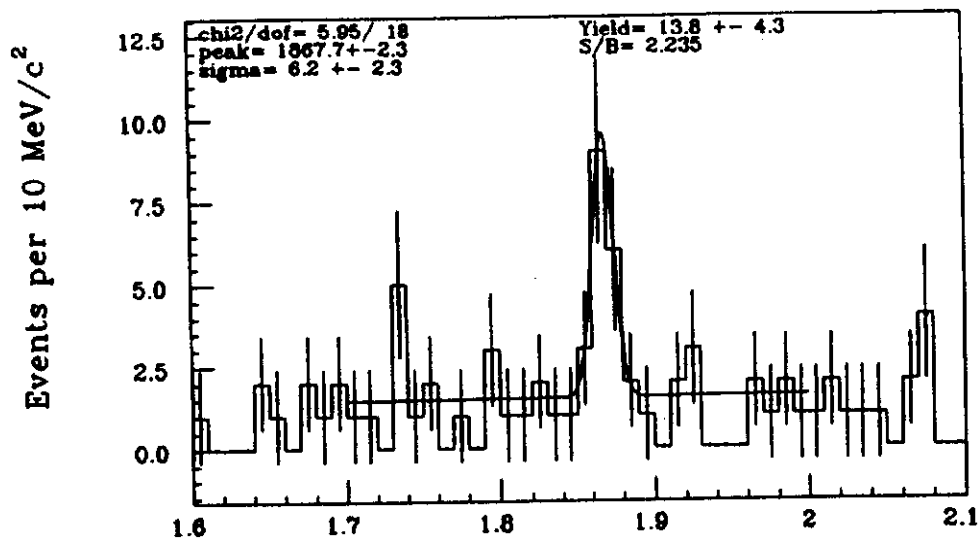Figure 2. W exchange diagram for $D^0 \rightarrow K^0\Phi$.

chi2/dof= 5.95/ 18
peak= 1867.7+−2.3
sigma= 6.2 +− 2.3

Yield= 13.8 +− 4.3
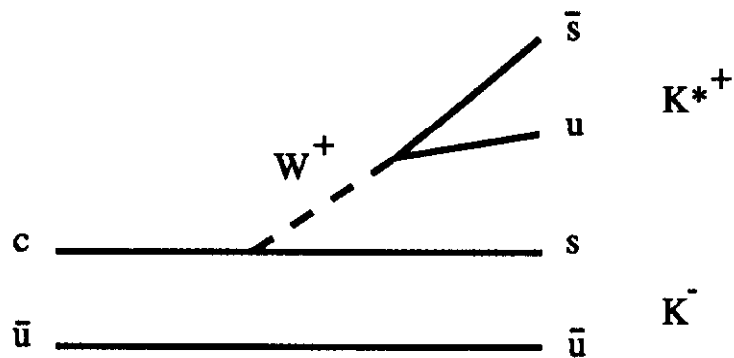S/B= 2.235

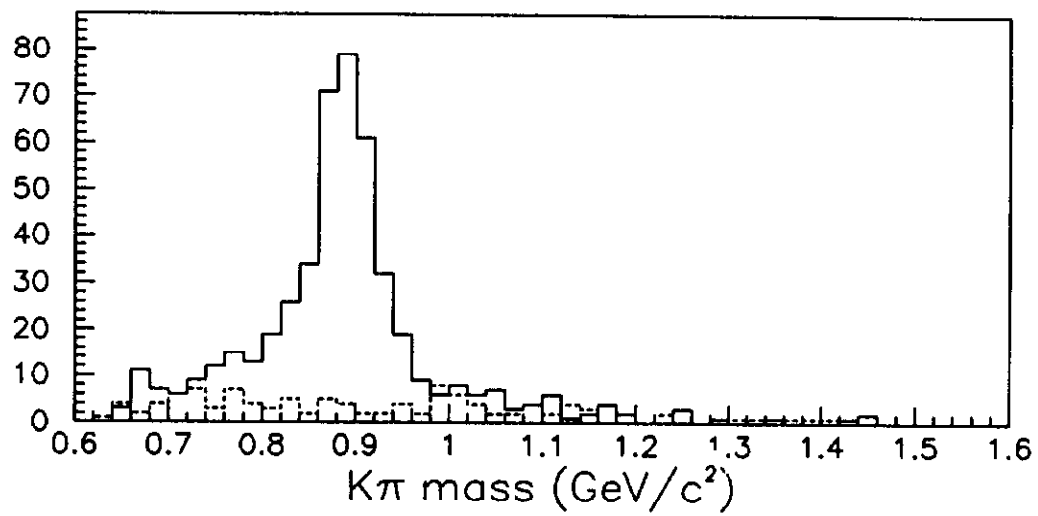Figure 3. $K^0_s \Phi$ invariant mass from E687.

Figure 4. Feynman diagram for $D0 \rightarrow K^{*+} K^-$

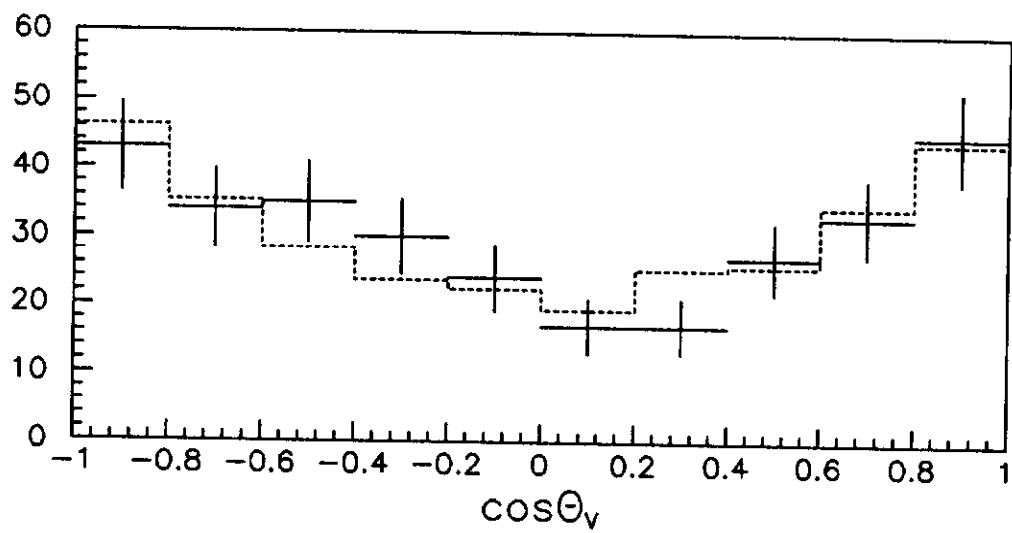Figure 5. $M_{K\pi}(GeV/c^2)$ for signal and wrong sign background from E653. This is typical of the quality of data in E653 and E687.

Figure 6. Uncorrected data and fit for θv from E653.
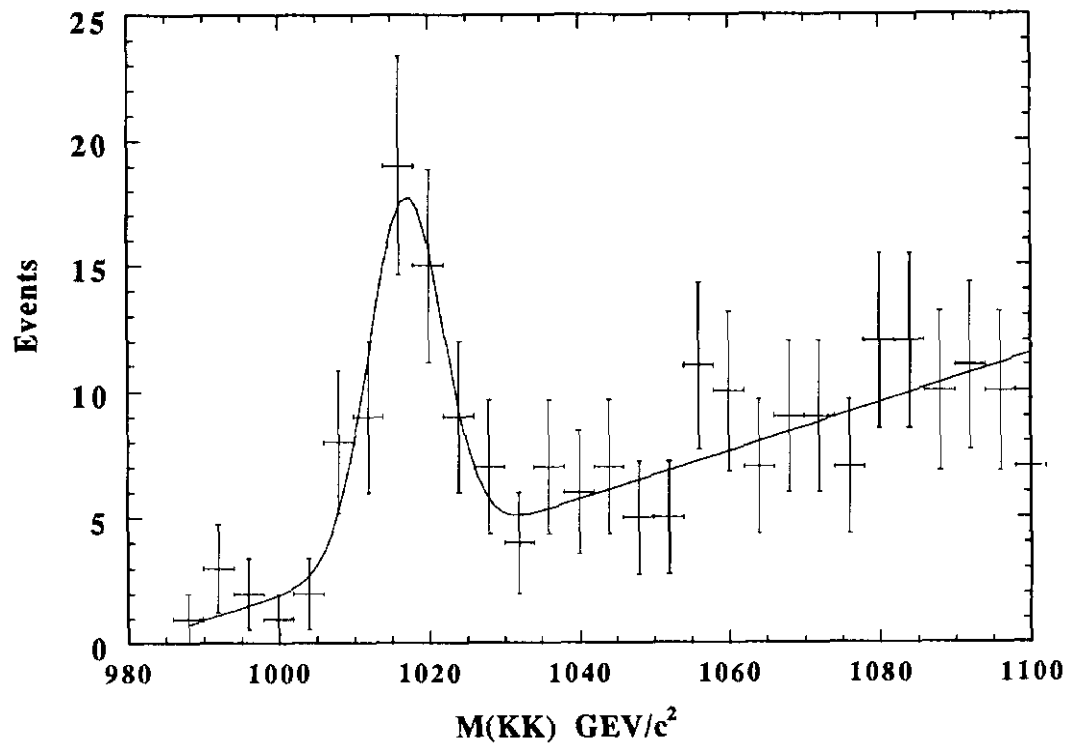
Figure 7. E653 $D_S \rightarrow \Phi\mu\nu$ signal. The solid curve is a fit to a Gaussian plus a polynomial background.
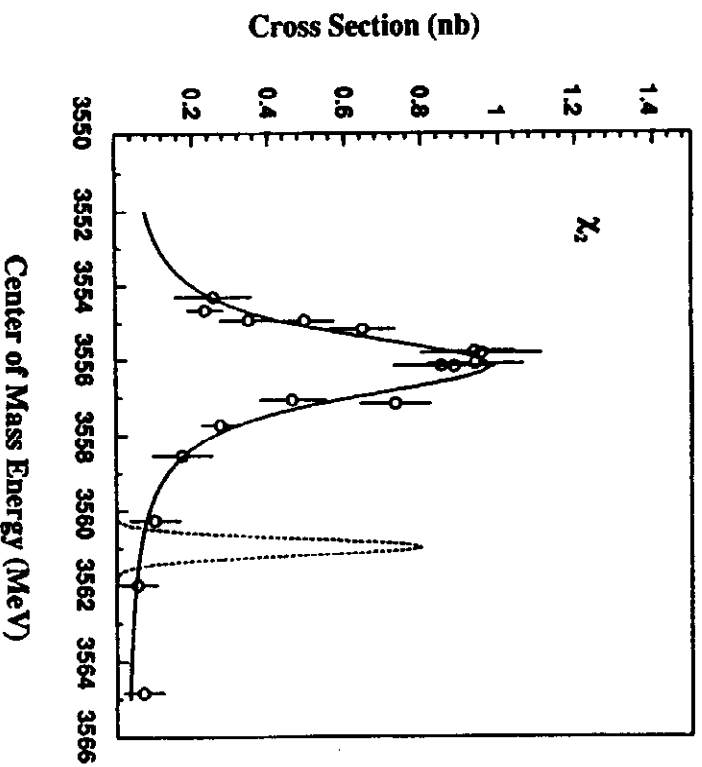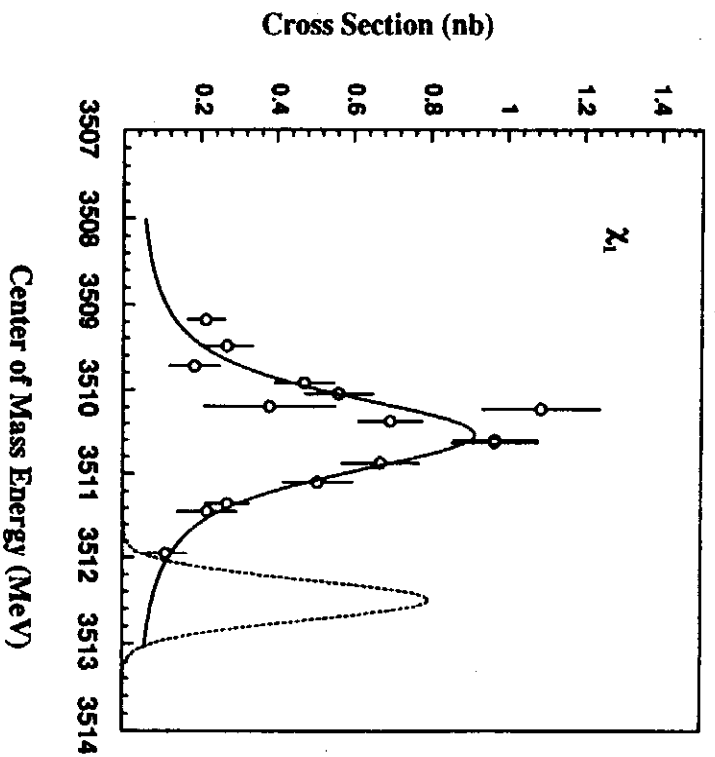
Figure 8. Measured cross section for energy scans at a) χ_1 and b) χ_2. The full line represents the best fit to the data. The dashed curve shows a typical center of mass energy distribution.
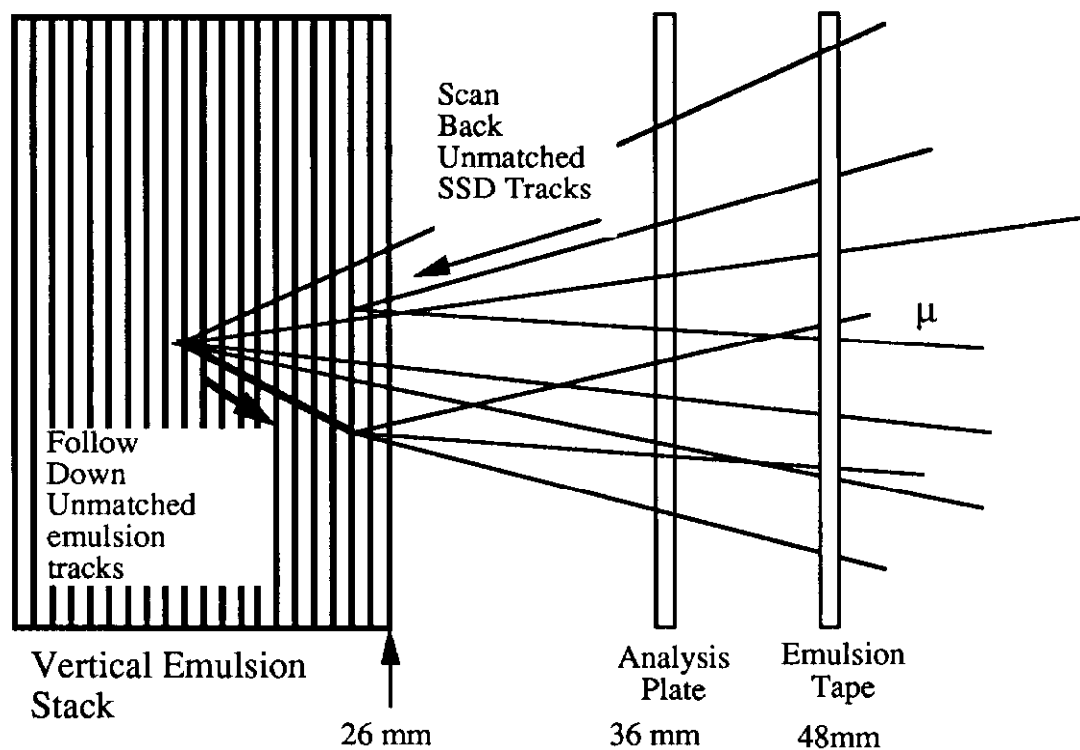
Figure 9. Schematic of the scanning technique in E653. The analysis plate is scaced out from the emulsion stack by low density foam. The emulsion tape moves continuously.
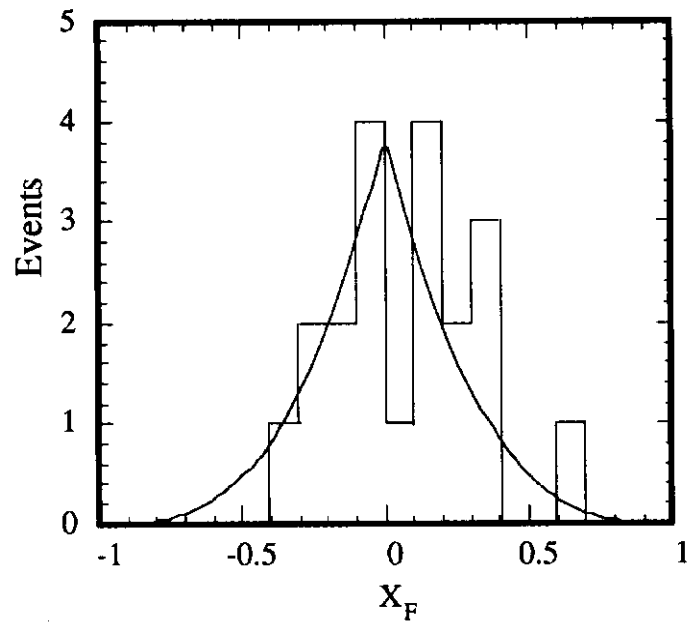
Figure 10. X_F distribution for the E653 B candidates. The solid line is a fit to $(1-X_F)^n$.
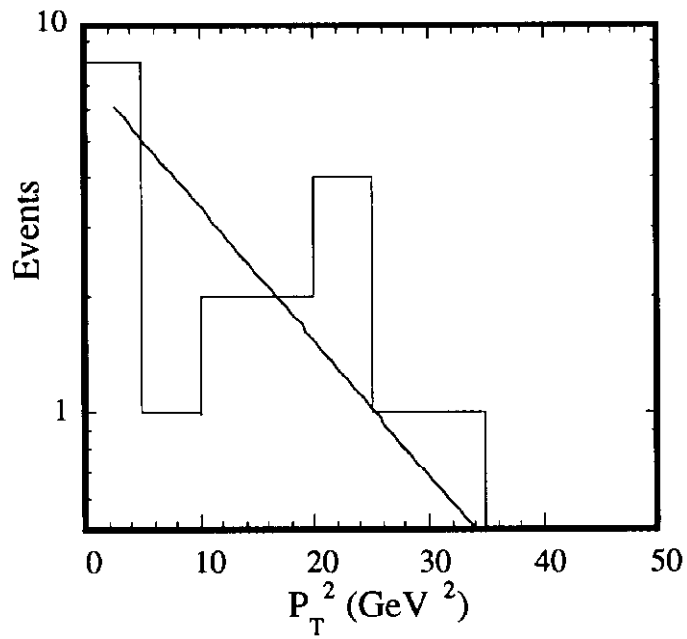

Figure 11. P_T^2 distribution for the E653 B candidates. The solid line is a fit to $e^{-bP_T^2}$.

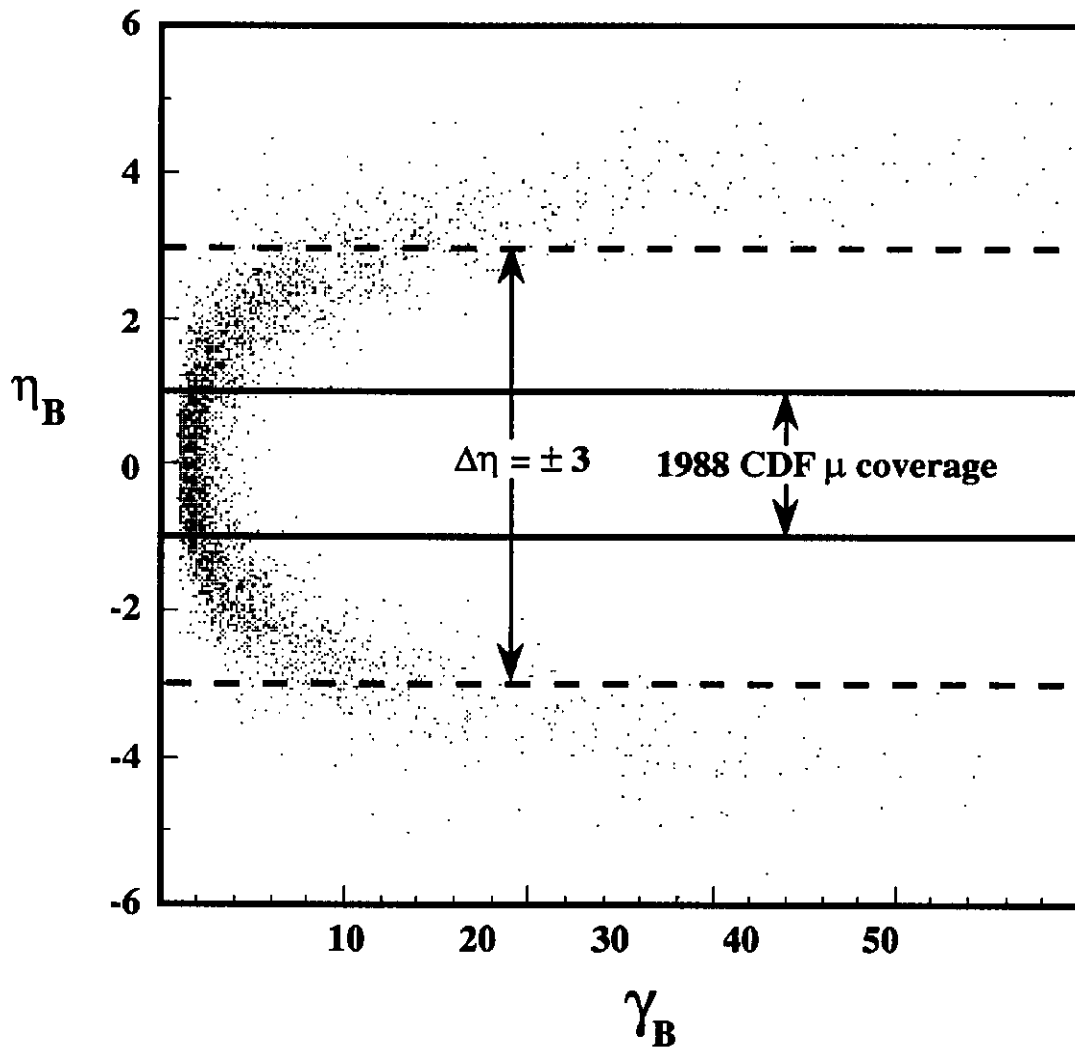The dashed line is typical of charm production.

Figure 12. Scatterplot of the Lorentz boost vs pseudorapidity for B's generated using ISAJET.
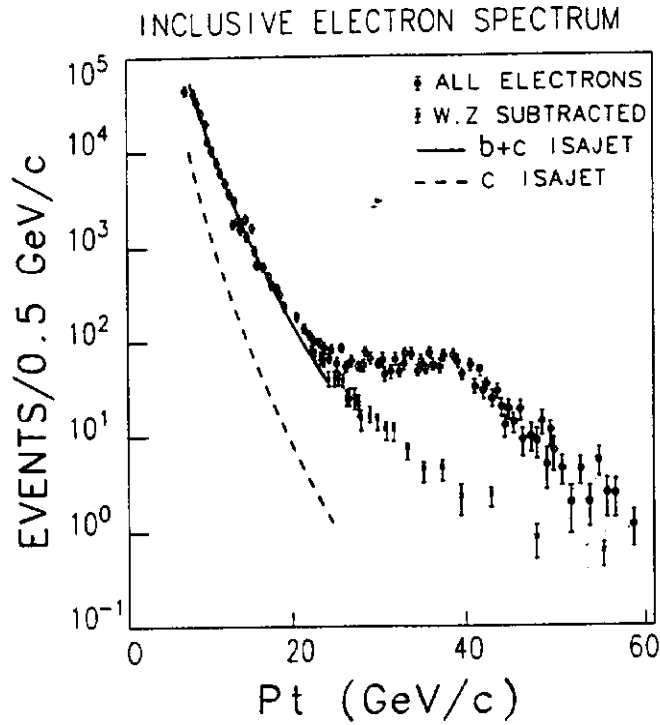
INCLUSIVE ELECTRON SPECTRUM

Figure 13. The inclusive electron spectrum for 1988-1989 CDF data. The circles are all electron candidates, the points are W and Z subtracted. Also shown is the ISAJET prediction for heavy quark production and decay.
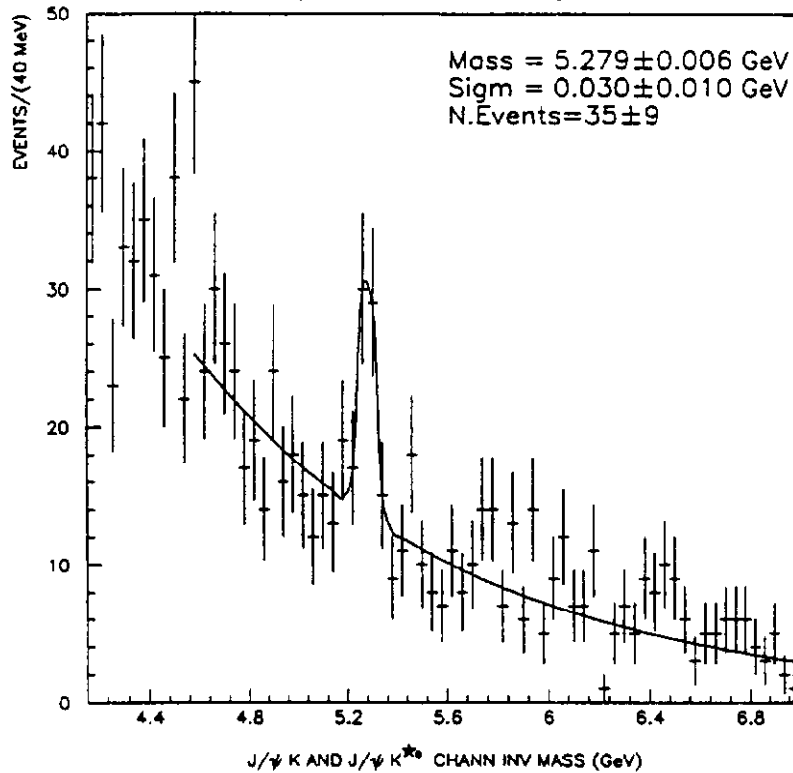

Mass = 5.279±0.006 GeV
Sigm = 0.030±0.010 GeV
N.Events=35±9

Figure 14. CDF data on $B \rightarrow J/\psi K^*$ and $B \rightarrow J/\psi K$

Kππ [KP7,DCL.L/σ>3]

500
400
300
200
100
0
1.7   1.8   1.9   2   2.1

M- 1.8638 ± .0018   Y-276.17 ± 45.90
W-10.155 ± 1.861   S/N-0.383880

Kππ [KP7,DCL.L/σ>5]

200
150
100
50
0
1.7   1.8   1.9   2   2.1

M- 1.8612 ± .0015   Y-224.59 ± 29.93
W-11.161 ± 1.589   S/N-0.955201

Kππ [KP7,DCL.L/σ>8]

150
100
50
0
1.7   1.8   1.9   2   2.1

M- 1.8626 ± .0014   Y-222.02 ± 22.77
W-12.541 ± 1.372   S/N- 2.06446

Kππ [KP7,DCL.L/σ>14]

80
60
40
20
0
1.7   1.8   1.9   2   2.1

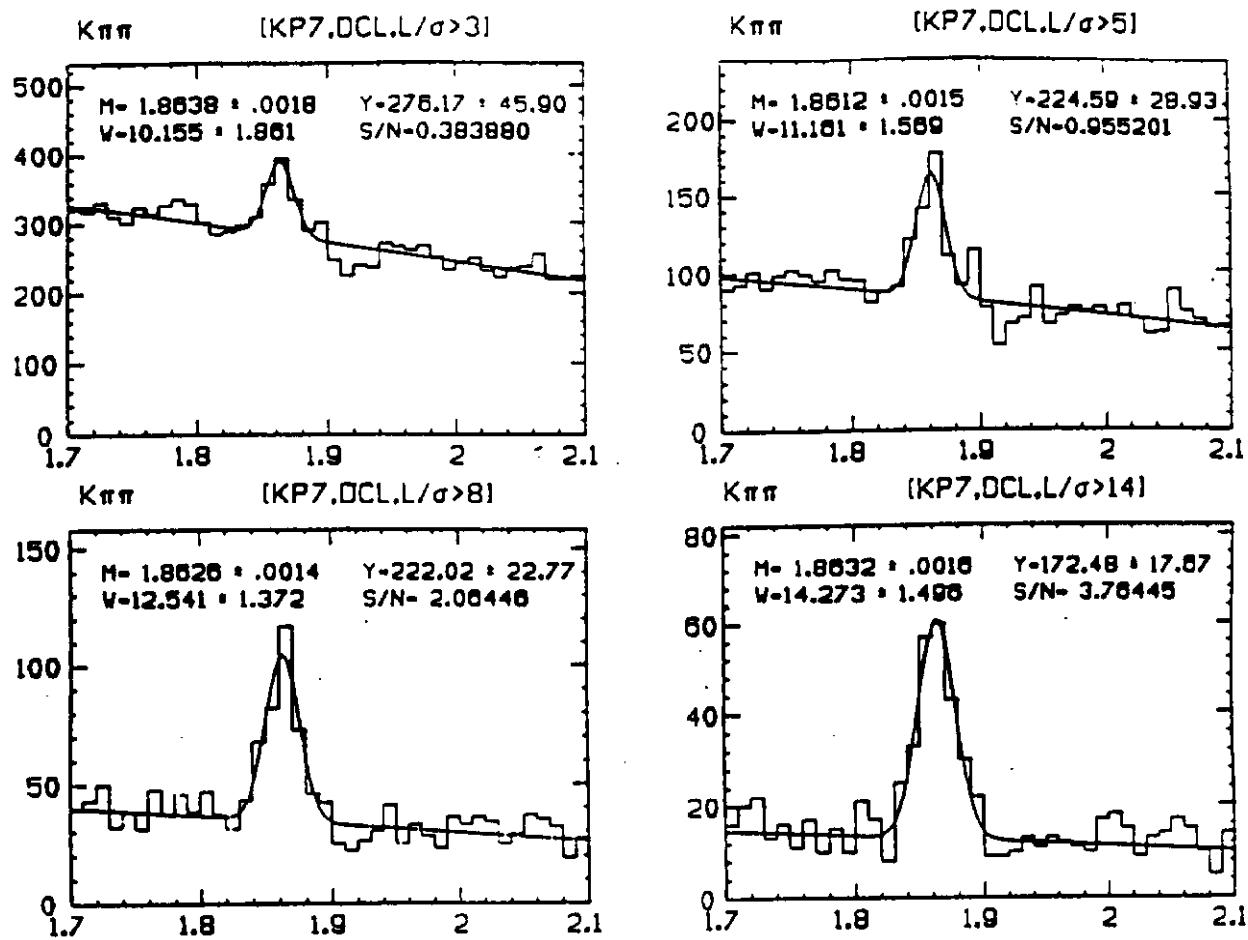M- 1.8632 ± .0016   Y-172.48 ± 17.67
W-14.273 ± 1.496   S/N- 3.76445

Figure 15. Charm signals in E687 from four shifts of data in the 1991 run.

1. The author has participated in experiment 653 and is currently collaborating on D0.

2. Judd Wilcox, Submitted to the DPF 1991, Vancouver, Canada.

3. Jeffrey Appel, FERMILAB-Conf-90/173.

4. S. Kwan, Proceedings of the 1990 SLAC Summer Institute.

5. P. Nanson and G. Rudolfi, private communication.

6. M.E. Duffy *et. al.*, Phys. Rev. Lett. **55**, 1816 (1985).

7. H. Cobbaert *et. al.*, Phys. Lett. **B206**, 546 (1988).

8. K. Kodama *et. al.*, Phys Lett **B263**, 579 (1991).

9. J.C. Anjos *et. al.*, Phys. Rev. Lett. **65**, 2503 (1990).

10. J.N. Butler, presented at the 1991 Lepton Photon Conference, Geneva,

    Switzerland.

11. J.C. Anjos *et. al.*, Fermilab Pub-90/183-E (Submitted to Phys Rev rapid. comm.)

12. J.C. Anjos *et. al.*, Fermilab Pub-91/147-E

13. P.L. Frabetti *et. al.*, Phys. Lett. **B263**, 584 (1991).

14. J.C. Anjos *et. al.*, Phys. Rev. Lett. **67**, 1507 (1991).

15. K. Kodama *et. al.*, Phys. Rev. Lett. **66**, 1819 (1991).

16. J.C. Anjos *et. al.*, Phys. Rev. Lett. **62**, 1587 (1989).

17. K. Kodama *et. al.*, in preparation and

    D. Gibaut, Submitted to the DPF 1991, Vancouver, Canada.

18 J.C. Anjos *et. al.*, Phys. Rev. Lett. **65**, 2630 (1990).

19 D.M. Potter, presented at the 1991 Lepton Photon Conference, Geneva,
    Switzerland.

20 F. Marchetto, Proceedings of the 4th Conference on Intersections between Particle
    and Nuclear Physics Tucson, USA, 1991.

21 T.A. Armstrong *et. al.*, submitted to Nuc. Phys. B.

22 C. Baglin *et. al.*, Nucl. Phys. **B286**, 592 (1987).

23. J.P. Albanese *et. al.*,Phys. Lett. **158B**, 186 (1985).

24. M.G. Catanesi *et. al.*,Phys. Lett. **187B**, 431 (1987).

25. E. Berger, Argonne Nat. Lab. ANL-HEP-CP-88-26.

26. A.R. Baden, Proceedings of the SLAC Summer Institute, 1990.

27. CDF Internal Note #1482.

28. D0 Upgrade Proposal, Fermilab.

29. N. Roe, D0 Internal Note #1022.

30. N. Roe, D0 Internal Note #1122.